Geosci. Instrum. Method. Data Syst., 9, 491–497, 2020
https://doi.org/10.5194/gi-9-491-2020

Geoscientific Instrumentation Methods and Data Systems
Open Access
EGU

Ground-penetrating radar inspection of subsurface historical structures at the baptism (El-Maghtas) site, Jordan

AbdEl-Rahman Abueladas and Emad Akawwi

Surveying and Geomatics Department, Faculty of Engineering, Al-Balqa Applied University, Al-Salt 19117, Jordan

Correspondence: AbdEl-Rahman Abueladas (aabueladas@bau.edu.jo)

Received: 30 May 2020 – Discussion started: 24 July 2020
Revised: 14 October 2020 – Accepted: 6 November 2020 – Published: 22 December 2020

Abstract. The baptism (El-Maghtas) site is located to the north of the Dead Sea on the eastern bank of the Jordan River. Previous archeological excavations in the surrounding area have uncovered artifacts that include the location that was home to "John the Baptist", who lived and preached in the early 1st Century AD and is known for baptizing Jesus. Archeological excavations have revealed walls, antiquities, and ancient water systems that include conduits, pools, and ancient pottery pipes. A ground-penetrating radar (GPR) survey was carried out at select locations along parallel profiles using a subsurface interface radar system (Geophysical Survey Systems Inc. SIRvoyer-20) with 400 MHz or 900 MHz mono-static shielded antennas in order to locate archeological materials at shallow depths. The GPR profiles revealed multiple subsurface anomalies across the study area. At the John the Baptist Church site a buried wall was detected along the profiles, and at the pool site the survey delineated several buried channels. GPR data also confirmed the extension of an ancient pottery pipe at the Elijah's Hill site through the production of a clear diffraction hyperbola anomaly related to the ancient pottery pipe that could be discriminated from the 2D profiles. The GPR data were displaced using 3D imaging to define the horizontal and vertical extent of the pipe.

1 Introduction

Locating an archeological site that contains buried artifacts and antiquities has traditionally involved methods such as coring, foretelling, and shovel testing, which are time-consuming and labor-intensive procedures that can lead to significant waste of time and expense. Ground-penetrating radar (GPR) is a unique high-resolution tool that offers a solution to these problems (Vaughan, 1986).

GPR uses electromagnetic (EM) waves with frequencies of 10–1000 MHz to picture subsurface soil and structure. It has become an accepted method for use in various fields, including archeology, geology, engineering and construction, environmental fields, and forensic science (Neal, 2004). The advantage of using EM waves with relatively short wavelengths lies in the ability to map small objects at shallow depth. This GPS methodology has been successfully utilized to locate antiquities in urban and arid settings (Vaughan, 1986; Sternberg and McGill, 1995; Cacione et al., 1996; Basile et al., 2000; Ronen et al., 2018) and has proven to be an efficient method for identifying areas with the highest potential for successful excavation (Cacione, 1996).

Additionally, GPR data presentations can play a significant role in archeological inspections since they provide a visual representation of the site, including the size and depth of any subsurface anomalies (Basile et al., 2000).

The main objective of this study is to carry out a GPR survey, which is a non-destructive and non-invasive method of obtaining information about the existence of archeological features in shallow subsoil and to image the extension of a partially excavated ancient pottery pipe. The baptism site is situated approximately 8 km from the northern corner of the Dead Sea on the eastern bank of the Jordan River (Fig. 1).

The site is located in an arid environment where a large number of archeological remains of various ages and sizes are located in variable geological–archeological media (Eppelbaum et al., 2010). Soils at the site are complex, and in some locations vegetation factors complicate the accessibility of a GPR survey (Eppelbaum and Khesin, 2001; Eppelbaum et al., 2010.

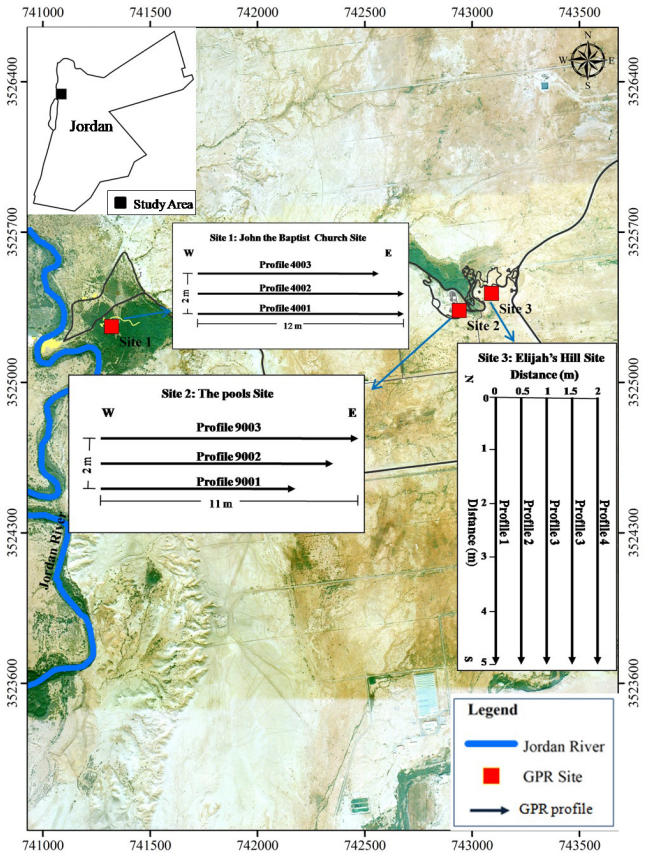

Figure 1. Location map of the GPR profiles study area "After © Google Earth".

The GPR survey was carried out at three different locations to identify any shallow anomalies.

2 Historical background

The baptism (El-Maghtas) site is a prehistoric area in Jordan Valley, about 50 km from Amman in western Jordan, with settlements within El-Maghtas known as Bethany in the place where John the Baptist lived in the time of Christ, making El-Maghtas one of the most important archeological sites associated with early Christianity.

John the Baptist's settlement is connected with several biblical events including the baptism of Jesus which took place in Bethany, Joshua's crossing of the Jordan River, the last days of Moses, and the Prophet Elijah's crossing of Jordan where he ascended to heaven in a whirlwind upon a chariot with horses of fire (2 Kings 2:5–14). For nearly 2000 years, local church traditions and pilgrimages have identified the small hill at the center of Bethany as the site from which Elijah was raised to paradise. The site became famous for this hill, Elijah's Hill (also Tell Mar Elias, Jabal Mar Elias), which is located 2 km west of the Jordan River.

The settlement of Bethany and surrounding regions in Jordan have been known by various names throughout history including Ainon, Saphsaphas, Bethanin, and Bethabra (Beit el-Obour, or house of the crossing). Arabic language bibles refer to it as Beit' Anya. Thus, today the entire region that falls between Bethany and the Jordan River is called El-Maghtas (the place of immersion or baptism).

Current archeological studies in the area have identified numerous structures, including monastic complexes, churches, caves, a system of water pipes, and channels as well as other facilities from the Roman and Byzantine era (4th to 8th centuries AD) (Waheeb, 2001). Effectively, these excavations have revealed a settlement from the time of Jesus and John the Baptist (early 1st century AD).

The existence of excavated water structures, such as aqueducts, pools, cisterns, and pottery pipes, attests to the complexity of the water system in the area. Previously settlers had depended on rainwater catchments and springs as sources of water, and the need for more water supplies prompted the Roman and Byzantine settlers to divert water from nearby Wadi using conduit and pottery pipes to fill pools and cisterns as reservoirs (Waheeb, 2003).

3 GPR concepts

GPR is a high-resolution method of imaging subsurface structures using EM waves with a frequency band from 10 MHz to 1 GHz. The benefit of using EM waves is that signals of a relatively short wavelength, which can be generated and directed to the subsurface to map anomalies, vary in their electrical properties in many aspects.

The horizontal resolution links to the ability to detect reflector location in space or time, which is a function of the pulse width. The vertical resolution increases with an increase in the frequency. The vertical resolution is also controlled by wavelength (λ) (Knapp, 1990), which is a function of velocity and frequency:

$$\lambda = v/f. \quad (1)$$

The best vertical resolution can be obtained by using one-quarter of the dominant wavelength (Sheriff, 1977).

4 GPR survey

A continuous GPR survey was conducted utilizing a SIRvoyer-20, produced by Geophysical Survey Systems, Inc. (GSSI). Antennas with 900 and 400 MHz frequency were used in this study. A total of 88 m of GPR surveys was conducted along 11 profiles at 3 different locations. The first survey location is located to the north of John the Baptist Church, the second is located to the south of the pools, and the third location is at Elijah's Hill.

Three profiles were conducted at each of the first two locations and five additional profiles were carried out on the

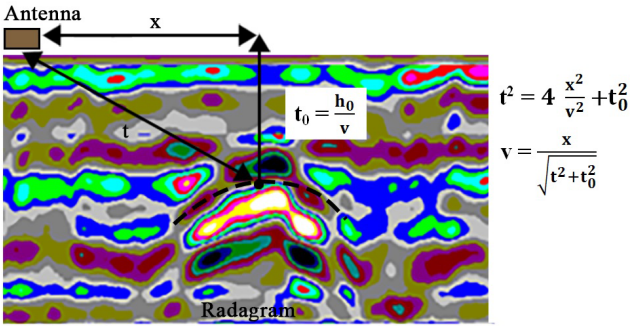

Figure 2. Hyperbolic reflections caused by pottery pipe is used to obtain the wave velocity with the equation of hyperbola.

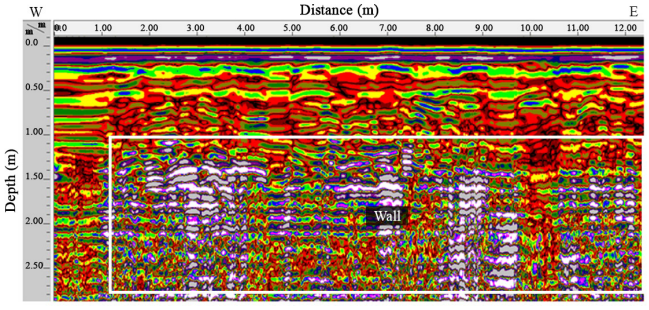

Figure 3. A 400 MHz antenna radargram along Profile 4001. The white rectangle along the radargram at approximate depth of 1.2 m may correspond to buried wall.

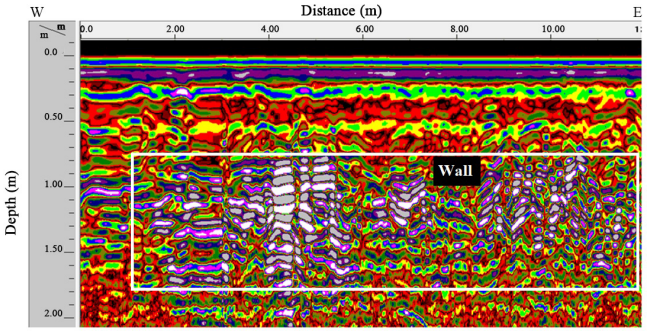

Figure 4. A 400 MHz antenna radargram along Profile 4002. The white rectangle along the radargram at approximate depth of 0.6 m may correspond to buried wall.

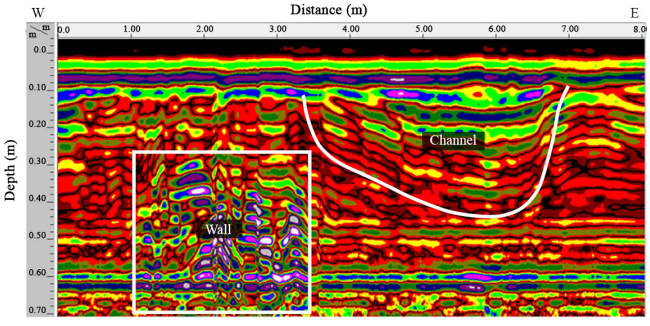

Figure 5. A 900 MHz antenna radargram along Profile 9001. The white rectangle along the radargram represents anomaly located between horizontal distance 1 and 3 m with approximate depth 0.25 m which may correspond to an ancient buried wall. The 4 m wide depression at end of the profile may be correlated to buried channel.

south side of at the third location at Elijah's Hill (Fig. 1). At the second and third sites, the surveys used a 900 MHz antenna.

Minimum data processing was applied to utilize the GSSI RADAN V software package from GSSI. Horizontal and vertical high- and low-pass filters have been applied to enhance the radar cross section and to eliminate the surplus noise from the GPR signal. Additional processing was used to convert two-way travel times along the section to depth in meters, applying average radar wave velocity. Data were stacked in the horizontal direction along with profiles. The data were then edited while both horizontal and vertical scales were attuned before processing (Abueladas, 2005).

Time-zero correction was applied to the raw GPR data, which were then managed using range and display gain, filtering, color conversion, and migration procedures (Aqeel et al., 2014).

The GPR data that were obtained were processed and presented as 2D depth cross sections providing a logical vertical and horizontal resolution for the uppermost 2 m of the inspected sites (Odah et al., 2013). Calculation of the subsurface radar-wave velocity is essential to convert the two-way travel time of the reflected signal to the real depth of the reflector (Annan, 2003; Fisher, 1992). However, this study calibrated the velocity according to the known depth aligned with the top of the excavated pipe near the study area.

The dielectric permittivity of the various areas was obtained using an approximation of the reflection delay formula, which connects wave velocity (v) to measured depth (x), the recorded two-way travel time (t), the relative permittivity (ξ_r), and the free-space velocity (c) (Gracia et al., 2008):

$$\xi_r = (c/v)^2 = (ct/2x)^2. \quad (2)$$

The computed near-surface average velocity was 0.12 m ns^{-1} (Fig. 2).

5 Results and discussion

Because of the lack of geophysical and archeological data for the study area, it was too difficult to interpret the GPR data.

A total of three continuous parallel profiles up to 12 m long were recorded at the site. The separation between the adjacent west–east profiles is constant at 1 m (Fig. 1).

The 400 MHz antenna radar gram along profile 4001 shows a large discontinuous linear anomaly at an approx-

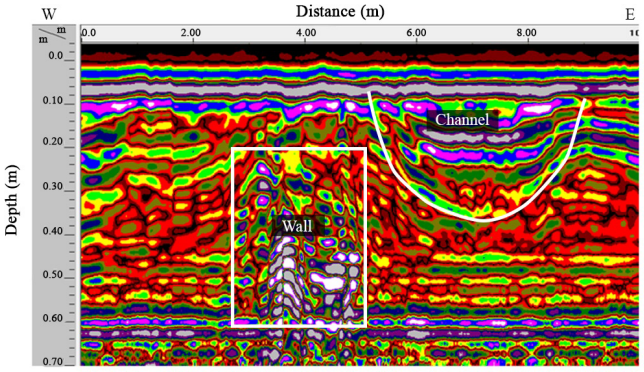

Figure 6. A 900 MHz antenna radargram along Profile 9002. The white rectangle along the radargram at approximate depth of 0.20 m may correspond to buried wall. The 4 m wide depression at end of the profile may be correlated to buried channel.

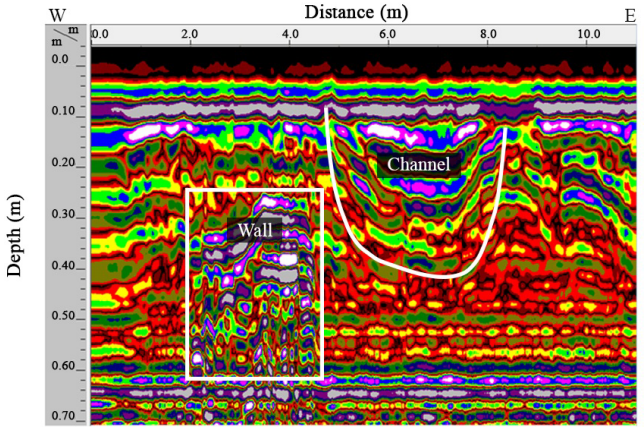

Figure 7. A 900 MHz antenna radargram along Profile 9003. The white rectangle along the radargram at approximate depth of 0.20 m may correspond to buried wall. The 4 m wide depression at end of the profile may be correlated to buried channel.

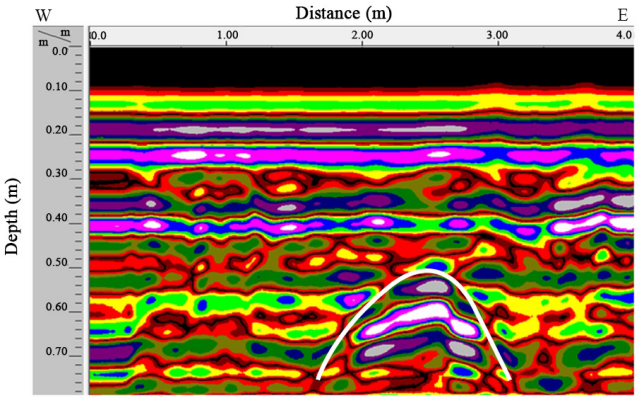

Figure 8. A part of 900 MHz antennae radargram along profile 1 immediately adjacent to excavated pottery pipe. The hyperbolic-shaped anomaly at distance 2.5 and 0.55 m deep shows the extension location of the buried pottery pipe.

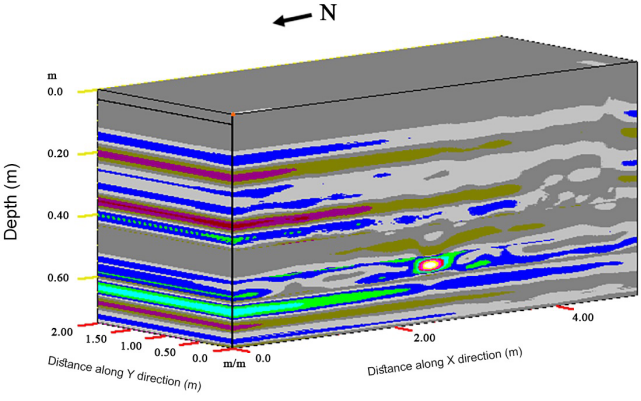

Figure 9. The 3D GPR data view constructed from 2D profile lines. The 3D perspective view of processed profiles using high pass and low pass vertical and horizontal filters together with migration technique that show the location of the pottery pipe.

imate depth of 1.2 m that is interpreted as a discontinuous buried wall and can be viewed in Fig. 3.

Profile 4002, which is located 1 m to the north, shows the same anomaly that was observed in profile 4001; however, it was detected at shallower depth (Fig. 4).

These anomalies are caused by dissimilarities in wave velocity at the point of contact between disparate materials. The depths and extensions of these anomalies most likely indicate the possibility that the buried wall with a north–south orientation is present in the subsurface. No other anomalies were detected within profile 4003.

A 900 MHz antenna with good spatial resolution was used at sites 2 and 3 and repeated. The GPR survey was performed along the profiles to provide more information about subsurface structures.

A 900 MHz antenna survey was conducted at site 2 along profile 9001 from west to east (Fig. 1). Figure 5 shows one primary anomaly at a depth of 0.25 m, located between the 1 and 3 m markers that are interpreted as a buried wall. The 3 m wide depression at the end of the profile may be correlated to a shallow buried channel.

Profile 9002 is 10 m long and runs parallel to profile 9001, approximately 1 m to the north (Fig. 1). The same anomaly and depression were detected along this profile as were found in profile 9001 (Fig. 6).

The 12 m long profile 9003 is located to the north of profile 9002 closer to the pool (Fig. 1). The radar profile shows an anomaly between the 2 and 5 m markers at an approximate depth of 0.25 m, which is interpreted as a buried wall (Fig. 7). The bottom of the depression along this profile is deeper, and the width is smaller than profiles to the south.

Site 3 is a 2 by 5 m rectangular section on a flat area near Elijah's Hill. The uni-directional survey was conducted along five profiles oriented approximately north–south and spaced

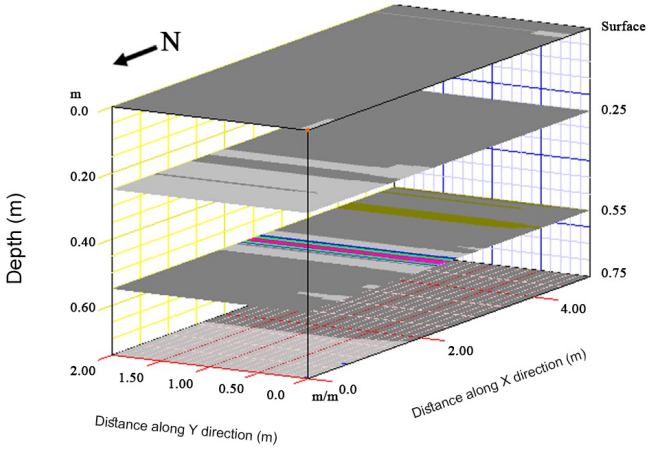

Figure 10. Depth slices with different depths (0, 025, 0,55, 0.75 m) generated from 3D plot . The main anomaly observed with W-E direction at depth slice 0.55 m b.s. (meter below surface).

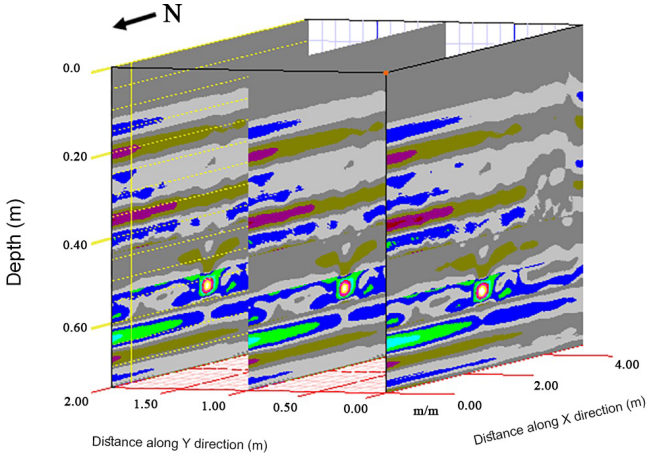

Figure 11. The multiple slices view along y direction at distance (0, 1 and 2 m) determines the depth and extension of the pipe.

0.5 m apart to the east of the excavated section of pottery pipe (Fig. 1).

The pottery pipe is one of the structures associated with an ancient water system. Most sections of this pipe were destroyed by human activities, but an intact segment was successfully excavated within the site.

GPR profile 1 was collected perpendicular to the trend of the excavated pottery pipe just east of the excavation using a 900 MHz antenna (Fig. 1). The hyperbolic-shaped anomaly appears at the 2.5 m mark and is about 0.55 m deep showing the location of the buried pipe (Fig. 8).

The main anomalies appear as diffraction hyperbolas with high amplitudes, observed at the 2.5 m marker and at 0.55 m depth, along the entirety of the 2D ground-penetrating radar cross section.

Generally, targets of interest are easier to identify using three-dimensional data rather than conventional two-

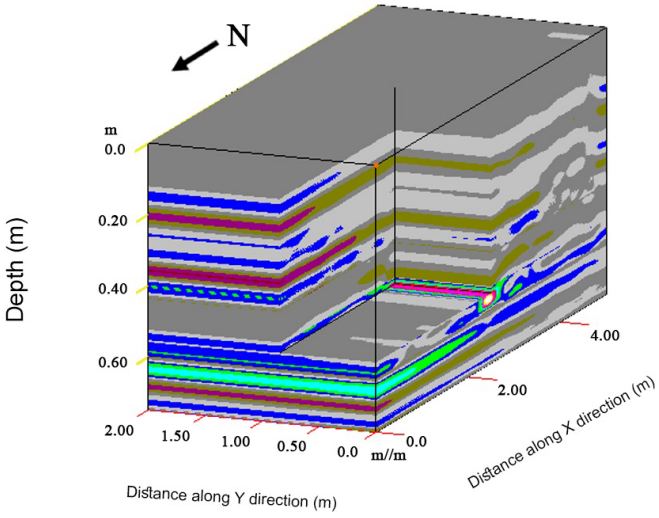

Figure 12. The 3D section (cutout cube) using $x = 2.5$, $y = 0.85$, and $z = 0.55$ m shows clearly the depth and extension of the pipe perpendicular to the x position and the depth of the top of pipe detect by the z position.

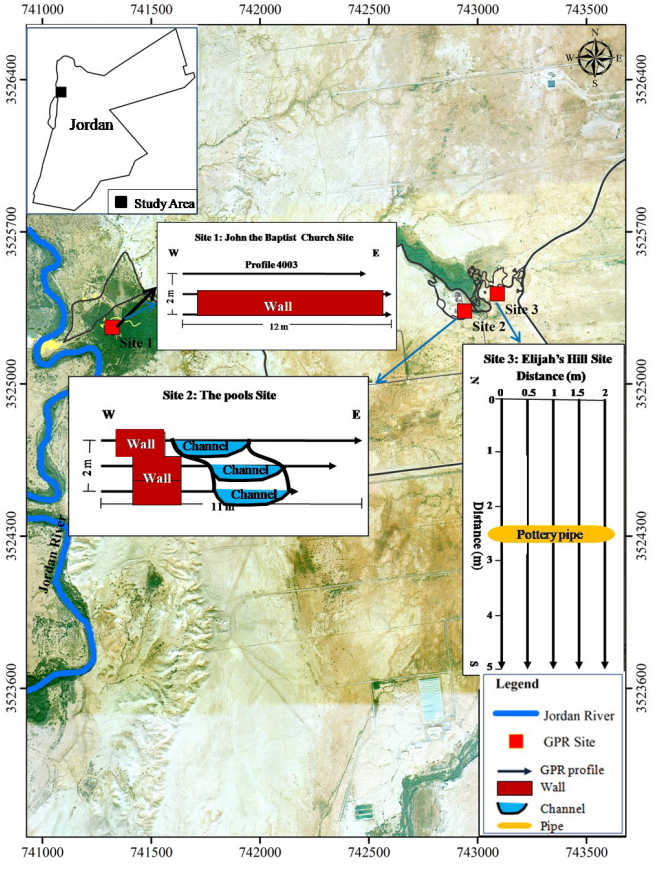

Figure 13. Location map of the inferred archeological material "After © Google Earth".

dimensional profile lines. The 3D GPR data were generated from two dimensions and displayed using 3D visualization techniques, which is of primary importance in archeological applications.

A 3D perspective of the processed profiles using high-pass and low-pass vertical and horizontal filters together with the migration technique illustrates the location of the pottery pipe (Fig. 9) (Whiting et al., 2001; Fisher, 1992).

Depth slices, which are useful for accurate interpretation, were generated at different depths (0, 0.25, 0.55, 0.75 m) from the 3D plot and are presented in Fig. 10. The main anomaly observed on the depth slice of 0.55 m b.s. (meters below the surface) has a west–east orientation and corresponds to the pottery pipe anomaly, which provides good information about the exact location and extension of the pipe.

The multiple-slice view along the y direction at various distances (0, 1, and 2 m) determines the extension of the pipe anomaly along the y direction (Fig. 11).

The 3D section (chair view) with $x = 2.5$, $y = 0.85$, and $z = 0.55$ m shows clearly the east–west extension of the pipe perpendicular to the x position, and the depth to the top of the pipe determined by the z position (Fig. 12). The results of this study showed that many subsurface structures were recognized using GPR. Subsurface walls were delineated and various subsurface channels were found.

The locations of these channels were well defined, and flow directions in these channels were also identified from west to east in the study area. Figure 13 shows the location map of GPR anomalies and their interpretation.

6 Conclusions

Ground-penetrating radar (GPR) is a powerful, non-destructive, non-invasive geophysical near-surface tool for archeological surveying. GPR has been used successfully in this study to detect several shallow anomalies at the El-Maghtas site. The flat topography and the absence of archeological features at the surface of the site allowed for collection of high-quality GPR data. The high-frequency 900 MHz antenna was successfully used to locate smaller archeological objects at shallow depths, and 3D images provided higher resolution than the 2D profiles, as can be seen from the results. Generally, the survey included the identification and mapping of covered walls, channels, and the extension of an ancient pottery pipe.

However, vertical sections, depth slices, and 3D images were used to locate the anomalies using a spatial-extent 3D survey, allowing for a precise detection of the anomaly throughout the surveyed data after advanced processing, including migration. The east–west-oriented extension of the pottery pipe at the El-Maghtas site was detected successfully by using three-dimensional GPR imaging.

The mapped archeological targets are relatively shallow, showing detectable anomalies from approximately 0.55 m below the ground surface extending to a depth of 1.2 m.

The displacement shown in the buried wall and channel in site 2 may be caused by a shallow fault. The results of this study can be used as a source for any future excavations.

Data availability. The raw data supporting the results and conclusions of this research are available from the authors upon request.

Author contributions. Both authors contributed to the conception and design of the study. ARA carried the field study and wrote the first draft of the article. EA contributed to the paper revision and approved the final submitted version.

Competing interests. The authors declare that they have no conflict of interest.

Acknowledgements. The authors would like to thank the Ministry of Higher Education and Scientific Research for their funding and support throughout the project. We would also like to thank Dia El-Madani, the former baptism site commission director, and his assistant Raslan Mkhjian for their help. We are also grateful to the technicians, Ibraheem Aldabas, Mohamed Aqrabawi, Zaid Heyassat, and the employees of Al-Balqa Applied University for their efforts during data acquisition and fieldwork. We thank the anonymous reviewers and the editor for their constructive criticism and comments on this paper very much.

Financial support. This research has been supported by the Scientific Research Support Fund, Ministry of Higher Education and Scientific Research, "Integration of Geometrics and Geophysics for Geospatial Archeology Database System in Jordan" (grant no. 1/60/2008).

Review statement. This paper was edited by Lev Eppelbaum and reviewed by two anonymous referees.

References

Abueladas, A.: Ground Penetrating Radar Investigations of Active Faults and Antiquities along the Dead Sea Transform in Aqaba and Taba Sabkha, Jordan, master thesis, University of Missouri-Kansas City, USA, 71 pp., 2005.

Annan, A. P.: GPR principles, procedures and applications: Sensors and Software In, 2003.

Aqeel, A., Anderson, N., and Maerz, N.: Mapping sub-vertical discontinuities in rock cuts using a 400-MHz ground penetrating radar antenna, Arab. J. Geosci., 7, 2093–2105, https://doi.org/10.1007/s12517-013-0937-y, 2014.

Basile, L., Carrozzo, M. T., Negri, S., Nuzzo, S., Quarta, L., and Villani, A. V.: A ground-penetrating radar survey for Archaeological investigations in an urban area (Lecce, Italy), J. Appl. Geophys., 44, 15–32, https://doi.org/10.1016/S0926-9851(99)00070-1, 2000.

Cacione, J. M.: Radar simulation for archaeological applications, Geophys. Prosp., 44, 871–888, https://doi.org/10.1111/j.1365-2478.1996.tb00178.x, 1996.

Eppelbaum, L. V. and Khesin, B. E.: Disturbing factors in geophysical investigations at archaeological sites and ways of their elimination, in: Transactions of the IV Conference on Archaeological Prospection, Vienna, Austria, 19–23 September 2001, 99–10, 2001.

Eppelbaum, L. V., Khesin, B. E., and Itkis, S. E.: Archaeological geophysics in arid environments: Examples from Israel, J. Arid Environ., 74, 849–860, https://doi.org/10.1016/j.jaridenv.2009.04.018, 2010.

Fisher, E.: Examples of reverse-time migration of single-channel, ground penetrating radar profiles, Geophysics, 57, 577–586, https://doi.org/10.1190/1.1443271, 1992.

Gracia, V., Garcí, F., Pujades, L., Drigo, R., and Capua, D.: GPR survey to study the restoration of a Roman monument, J. Cult. Herit., 9, 89–96, https://doi.org/10.1016/j.culher.2007.09.003, 2008.

Knapp, R. W.: Vertical resolution of thick beds, thin beds and thin-bed cyclothems, Geophysics, 55, 1183–119, https://doi.org/10.1190/1.1442934, 1990.

Neal, A.: Ground-penetrating radar and its use in sedimentology: principles, problems and progress, Earth-Sci. Rev., 6, 261–330, https://doi.org/10.1016/j.earscirev.2004.01.004, 2004.

Odah, H., Ismail, A., Elhemaly, I., Anderson, N., Abbas, A., and Shaaban, F.: Archaeological exploration using magnetic and GPR methods at the first court of Hatshepsut Temple in Luxor, Egypt, Arab. J. Geosci., 6, 865–871, https://doi.org/10.1007/s12517-011-0380-x, 2014.

Ronen, A., Ezersky, M., Beck, A., Gatenio, B., and Simhayov, R. B.: Use of GPR method for prediction of sinkholes formation along the Dead Sea Shores, Israel, Geomorphology, 328, 28–43, https://doi.org/10.1016/j.geomorph.2018.11.030, 2018.

Sheriff, R. E.: Limitations on resolution of seismic reflections and geologic detail derivable from them, Appl. Geophys., 20, 3–14, 1977.

Sternberg, B. K. and McGill, J. W.: Archaeology studies in southern Arizona using ground penetrating radar, J. Appl. Geophys., 33, 209–225, https://doi.org/10.1016/0926-9851(95)90042-X, 1995.

Vaughan, C. J.: Ground penetrating radar survey used in archaeological investigations, Geophysics, 51, 595–604, https://doi.org/10.1190/1.1442114, 1986.

Waheeb, M.: Archaeological Excavations at the Baptism Site, Bethany Beyond the Jordan, Bible Spade, 14, 43–53, 2001.

Waheeb, M.: Recent Discoveries in the Bethany Beyond Jordan in Jordan Valley, Annual of the Department of Antiquities of Jordan, 47, 243–246, 2003.

Whiting, B., McFarland, D., and Hackenberger, S.: Thee-Dimensional GPR study of a prehistoric site in Barbados, West Indies, J. Appl. Geophys., 47, 217–226, https://doi.org/10.1016/S0926-9851(01)00066-0, 2001.